Molecular Biology of the Cell
Vol. 16, 193–201, January 2005

Anillin Binds Nonmuscle Myosin II and Regulates the Contractile Ring[D] [V]

Aaron F. Straight,*† Christine M. Field,‡ and Timothy J. Mitchison‡

*Department of Biochemistry, Stanford University School of Medicine, Stanford, CA 94305; and ‡Department of Systems Biology, Harvard Medical School, Boston, MA 02115

Submitted August 31, 2004; Revised October 6, 2004; Accepted October 8, 2004
Monitoring Editor: Yixian Zheng

We demonstrate that the contractile ring protein anillin interacts directly with nonmuscle myosin II and that this interaction is regulated by myosin light chain phosphorylation. We show that despite their interaction, anillin and myosin II are independently targeted to the contractile ring. Depletion of anillin in *Drosophila* or human cultured cells results in cytokinesis failure. Human cells depleted for anillin fail to properly regulate contraction by myosin II late in cytokinesis and fail in abscission. We propose a role for anillin in spatially regulating the contractile activity of myosin II during cytokinesis.

INTRODUCTION

During cytokinesis the site of cell division is determined by the position of the mitotic spindle, and beginning in anaphase, the contractile ring is assembled midway between the spindle poles. The cell is then divided by contraction of the cleavage furrow followed by the insertion of a membrane barrier at the site of contraction (Straight and Field, 2000; Glotzer, 2001).

Cytokinesis has been extensively described by observation and mutational analysis and many of the proteins that comprise and regulate the behavior of the contractile apparatus have been identified (Rappaport, 1996), but we do not yet understand the biochemical function of many cytokinesis proteins nor how they work together. Inhibition of proteins important for cytokinesis, either genetically or biochemically, typically produces two general effects: 1) inhibition of furrow ingression and 2) partial or full ingression of the furrow followed by furrow regression.

The first class, a block to furrow ingression, can result from preventing the assembly of the furrow or from blocking the contraction of the contractile apparatus. A classical example of this is the inhibition of either nonmuscle myosin II or actin that are necessary for contraction of the cytokinetic ring. Genetic deletion of myosin or biochemical inhibition of its contractile activity causes a failure in cytokinesis due to the absence of furrow contraction (Mabuchi and Okuno, 1977; De Lozanne and Spudich, 1987; Knecht and Loomis, 1987; Straight *et al*., 2003).

The second class, regression of the cleavage furrow late in cytokinesis, may result from either failing to maintain furrow contraction or failing to introduce a new membrane barrier between daughter cells. Inhibition of many proteins involved in cytokinesis results in this phenotype, including proteins important for the cytoskeleton, proteins controlling membrane dynamics, and signaling molecules (Straight and Field, 2000). Although these early and late phenotypes represent distinct steps in cytokinesis, they must be intimately coupled

The contractile ring protein anillin has been shown to be involved in cytokinesis via antibody injection in vertebrate cells and RNA interference (RNAi) in cultured *Drosophila* cells (Oegema *et al*., 2000; Somma *et al*., 2002). The anillin inhibition phenotype fits class 2 described above in that furrows ingress but completion of cleavage fails. Anillin has been shown to bind and bundle actin filaments and in vitro can provide a link between the actin cytoskeleton and another cytoskeletal complex important for cytokinesis, the septins (Field and Alberts, 1995; Kinoshita *et al*., 2002). However, we do not currently understand anillin's function during cytokinesis.

Here, we investigated the function of anillin in cytokinesis by using biochemistry, cytology, and RNA interference. We show that anillin specifically binds to activated nonmuscle myosin II and helps to focus myosin at the contractile ring. Although nonmuscle myosin II and anillin are both assembled into the contractile ring early in cytokinesis, we demonstrate that they are targeted there independently. In anillin-depleted cells, myosin II contraction late in cytokinesis is no longer constrained to the cleavage furrow, resulting in disorganized contractility and cytokinesis failure. We propose that anillin is required late in cytokinesis to localize the contractile activity of myosin.

MATERIALS AND METHODS

Cloning of Xenopus Anillin

Xenopus laevis anillin was cloned by degenerate polymerase chain reaction (PCR) from a *Xenopus* ovary cDNA library based upon the highly conserved PH domain of Human and *Drosophila* anillin proteins by using the primers 5′-TAYTGGAMNTAYCCNGAYGAYGA-3′ and 5′-YTCYTCYTTNGTRTC-NGC-3′. The full-length *Xenopus* anillin was then isolated by hybridization screening of the same library. The sequence of the full-length clone has been deposited as GenBank accession no. AY180201.

Constructs for RNA-mediated Inhibition

A T7 promoter flanked clone of the 5′ untranslated region and 460 nucleotides of the coding region of *Drosophila* anillin was cloned by reverse transcription-

Article published online ahead of print. Mol. Biol. Cell 10.1091/mbc.E04–08–0758. Article and publication date are available at www.molbiolcell.org/cgi/doi/10.1091/mbc.E04–08–0758.

[D] [V] The online version of this article contains supplemental material at MBC Online (http://www.molbiolcell.org).

† Corresponding author. E-mail address: astraight@stanford.edu.

PCR into pZeroBlunt (Invitrogen, Carlsbad, CA) by using the oligonucleotides 5′-GAATTAATACGACTCACTATAGGGAGAGCGCGTCGTTTTGAAATTATTC-3′ and 5′-GAATTAATACGACTCACTATAGGGAGACCCATGCGTTGCAGTCGGCTGCG-3′ to yield pAFS279. An analogous approach was taken for the nonmuscle myosin II heavy chain gene. A fragment of the nonmuscle myosin II coding region was amplified using the primers 5′-GAATTAATACGACTCACTATAGGGAGAATGTCGGAGGAAGTAGATCGCAACGATCCG-3′ and 5′-GAATTAATACGACTCACTATAGGGAGAAATGAGCACGGCGGGATGCGGCACCGCACC-3′. This fragment is expressed in all known splice variants of *Drosophila* nonmuscle myosin II (Mansfield *et al*., 1996). Double-stranded RNA was produced by transcription using Megascript-T7 (Ambion, Austin, TX) according to the manufacturer's instructions.

Human anillin small interfering RNA (siRNA) duplexes with the following sequences recognizing the human anillin coding region were used: siRNA1 in Figure 8A, AAGCGAGCUAGACAGCCACUU; siRNA2 in Figure 8A, GCAACUGCAGCCUCCUCAG; for nonanillin control siRNA, we used AUGUACCGGGUGGGAGAUU. The short hairpin RNA (shRNA) sequence 5′-TGCAACTGCAGCCTCCTCAGTTCAAGAGACTGAGGAGGCTGCAGTTGCTTTTTTCTCGA-3′ was cloned into the *Hpa*I-*Xho*I sites of pLL3.7 (a generous gift of Luk van Parijs, Massachusetts Institute of Technology). The green fluorescent protein (GFP) sequence in this plasmid or in the parent pLL3.7 was then replaced with yellow fluorescent protein (YFP)-Myosin regulatory light chain (RLC) to yield plasmids ASP446 and ASP445, respectively. For live cell imaging experiments, these constructs were cotransfected with siRNA duplexes. This ensured depletion and marked shRNA transfectants with the YFP-Myosin RLC construct.

Protein Expression and Antibody Production

To generate anillin-specific antibodies, a fragment of anillin spanning amino acids 436–717 was cloned by PCR by using primers 5′-CGCGGATCCCGGGGACGATATGACCGTCG-3′ and 5′-CCTGCAGTCGACGGTCTTCATTTTTTGTTTG-3′ digested with *Bam*HI and *Sal*I and fused to glutathione *S*-transferase (GST) by ligation into pGEX-6P-1 to yield pAFS209. GST fusions were expressed in *Escherichia coli* and purified on glutathione agarose and antibodies were produced in rabbits. Antibodies were affinity purified against the original antigen after depletion of GST-specific antibodies. *Xenopus* myosin II heavy chain-specific antibodies were prepared as described previously (Kelley *et al*., 1996) and affinity purified against the immunogenic peptide. Antibodies to *Drosophila* myosin II and anillin have been reported previously (Field and Alberts, 1995).

Full-length *Xenopus* anillin was cloned into pFastBac-HTa to yield pAFS217. Truncations of anillin were constructed as follows: 1–747 represents the *Bam*HI fragment of anillin cloned into pFastBac-HTa (pAFS215), 1–517 was constructed by *Xba*I digestion of pAFS215 and religation (pAFS224), 1–418 was constructed by *Nhe*I-*Xba*I digestion of pAFS215 and religation (pAFS223), 1–254 was constructed by *Stu*I digestion of pAFS215 and religation (pAFS222), and 1–142 was constructed by *Hind*III digestion and religation of pAFS215 (pAFS221). The anillin pleckstrin homology (PH) domain was amplified by PCR by using primers 5′-GCCATGTGAATTCTTCTGTTG-3′ and 5′-GCGCTCTAGATTACCACATTCGGAGATCCAC-3′, digested with *Eco*RI and *Xba*I and ligated into pFastBac-HTc (pAFS225).

To express *Xenopus* myosin II, the *Nco*I-*Eco*RI fragment of *Xenopus* myosin IIA (Bhatia-Dey *et al*., 1998) was cloned into pFastBac-HTa. This fragment generates the heavy meromyosin equivalent of the myosin II heavy chain. Coexpression of the truncated myosin II heavy chain and the essential and regulatory light chains was accomplished by coinfection of the heavy chain virus with a virus encoding the essential and regulatory light chains (Pato *et al*., 1996). Recombinant baculoviruses were produced and protein expressed according to the manufacturer's instructions (Invitrogen).

Proteins were purified from *Spodoptera frugiperda* (Sf9) cells by extraction with column buffer (0.5 M KCl, 20 mM KPO_4, pH 7.2, 10 mM imidazole, and 5 mM β-mercaptoethanol) containing 1 mM phenylmethylsulfonyl fluoride (PMSF), 10 μg/ml each leupeptin, pepstatin, and chymostatin [LPC] and 1% IGEPAL-CA630). Extracts were centrifuged for 1 h at 100,000 $\times$ *g*, and then the supernatant was bound to Ni-NTA agarose (QIAGEN, Valencia, CA). Resin was washed with 50 volumes column buffer containing 10 μg/ml LPC and 10% glycerol, 50 volumes of the same buffer at pH 6.0, and then eluted using column buffer containing 10% glycerol and 300 mM imidazole at pH 7.2. Proteins were then further purified by chromatography on S-Sepharose (Pharmacia, Uppsala, Sweden) by using a linear gradient from 20 to 500 mM KCl in 10 mM PIPES, pH 6.8, and 10% glycerol.

Human platelet nonmuscle myosin II was purified as described previously (Daniel and Sellers, 1992). Myosin II was further purified by gel filtration through KI and Mg-ATP to remove residual actin (Pollard, 1982). Myosin light chain kinase was purified from chicken gizzard according to the method of Walsh *et al*. (1983), and actin was purified from rabbit skeletal muscle (Pardee and Spudich, 1982). Recombinant human heavy meromyosin was expressed in Sf9 cells as described previously (Wang *et al*., 2000).

Immunoprecipitation

Eight micrograms rabbit IgG or anti-anillin antibody were bound to 25 μl of Affiprep protein A beads in 150 mM NaCl, 20 mM Tris-HCl, pH 7.4, and 0.1% Triton X-100 for 1 h at 4°C. The beads were split into two tubes each, and 200 μl of either crude cytostatic factor (CSF) arrested extract or activated interphase extract (prepared as described previously; Murray, 1991) was added. After 1 h at 4°C, the beads were harvested by centrifugation, washed five times with an excess of extract buffer, and boiled in Laemmli sample buffer. Immunoprecipitates were separated by SDS-PAGE and blotted with anti-actin antibody (Roche Diagnostics, Indianapolis, IN).

Affinity Chromatography

Purified anillin protein was dialyzed into coupling buffer (0.5M KCl, 20 mM HEPES, pH 7.7, and 10% glycerol) and coupled to Affigel-10 (Bio-Rad, Hercules, CA). Coupling was monitored until 75–80% coupling was achieved then quenched with 50 mM ethanolamine at pH 9.3.

Mitotic and interphase *Xenopus* extracts were prepared as described previously (Murray, 1991) with the following modifications. Microcystin-LR was added to mitotic extracts to prevent release into interphase. Interphase extracts were made from eggs activated with 1 μg/ml calcium ionophore A23187. Extracts were diluted five- to sevenfold into affinity column buffer (50 mM HEPES. pH 7.7, 100 mM KCl, 1 mM EGTA, 10 mM $MgCl_2$, and 1 mM dithiothreitol [DTT]) containing 1 mM PMSF, 10 μg/ml LPC, and ATP-regenerating system (7.5 mM creatine phosphate, 1 mM ATP, 0.1 mM EGTA, and 1 mM $MgCl_2$), and for mitotic extracts 1 μM microcystin-LR. Extracts were centrifuged for 1 h and 40 min at 200,000 $\times$ *g*, passed through a column of immobilized bovine serum albumin (BSA) to decrease nonspecific binding, and then applied to anillin affinity columns equilibrated in affinity column buffer. Columns were washed with 10 column volumes of column buffer and eluted with 100 mM increments of KCl in affinity column buffer. Eluates were precipitated with 10% trichloroacetic acid, and approximately one-third of the total eluate was separated by SDS-PAGE and stained with Coomassie Brilliant Blue.

Myosin Binding Assay

Purified human platelet myosin (5 μg) was phosphorylated with either 160 ng of Polo kinase, 380 ng of myosin light chain kinase, or 500 ng of CyclinB/CDC2 kinase in 50 μl of kinase buffer (50 mM Tris, pH 7.0, 50 mM KCl, 10 mM $MgCl_2$, 1 mM ATP, 1 mM DTT, and 0.2 mM $CaCl_2$) for 30 min at 30°C. The myosin light chain kinase reaction also contained 1 μg of calmodulin. Fifty microliters of beads with covalently coupled full-length anillin or GST was blocked in binding buffer (50 mM Tris, pH 7.0, 50 mM KCl, 10 mM $MgCl_2$, 1 mM DTT, and 0.1% Tween 20) containing 100 μg/ml BSA. One-half of each kinase reaction was then added to the beads and incubated with mixing for 1 h at 4°C. Beads were washed four times in an excess of binding buffer, boiled in Laemmli sample buffer, and separated on SDS-PAGE gels. Myosin II association was detected by both Coomassie Blue staining and by Western blotting.

Immunofluorescence

Xenopus tissue culture cells were fixed in cytoskeleton buffer with sucrose (10 mM MES, pH 6.1, 138 mM KCl, 3 mM $MgCl_2$, 2 mM EGTA, and 0.224 M sucrose [70% tonicity for *Xenopus* cells]) containing 4% formaldehyde for 20 min at room temperature. Cells were washed in 150 mM NaCl and 20 mM Tris-Cl, pH 7.4 (TBS) and then permeabilized for 10 min in TBS containing 0.5% Triton X-100. Cells were then washed in TBS containing 0.1% Triton X-100 and blocked in antibody dilution buffer (TBS, 0.1% Triton X-100, 2% BSA, and 0.1% NaN_3). All antibody incubations were performed in antibody dilution buffer. *Drosophila* tissue culture cells were fixed as described previously (Wheatley *et al*., 1998) to optimally preserve myosin II staining. HeLa cells were fixed in 80 mM K^+-PIPES, pH 6.8, 1 mM $MgCl_2$, 10 mM EGTA, 0.1% Triton X-100, and 4% formaldehyde for 15 min at 37°C and stained as described previously (Straight *et al*., 2003).

Drosophila *Cell Double-stranded RNA (dsRNA) Inhibition*

Logarithmically growing *Drosophila* Kc167 cells were harvested, washed in serum-free DES media (Invitrogen), and diluted to a concentration of 2.5 $\times$ 10^6 cells/ml. For each dsRNA treatment, 200 μl of cells were added to dsRNA to yield a final concentration of 75–100 nm of RNA. After 30 min of incubation at room temperature, cells were plated into wells of a 24-well dish, and 800 μl of complete Schneider's *Drosophila* media was added to the wells. After 56–72 h, 10% of the cells were replated onto 18-mm poly-L-lysine–coated coverslips and allowed to adhere for 3 h, whereas the remaining cells were processed verification of protein depletion by Western blotting. After 3 h, cells were fixed as described above and stained for relevant antigens. Myosin II dsRNA inhibition required replating cells at 72 h and a further incubation for 72 h before the bulk of myosin II had been depleted.

HeLa Cell siRNA Inhibition

HeLa cells growing in DMEM with 10% fetal bovine serum (FBS) were plated in 24-well plates at 5 $\times$ 10^4 cells/well. For siRNA treatment, 3 μl of 20 μM siRNA duplex was diluted in 50 μl of Optimem-I (Invitrogen), and 3 μl of

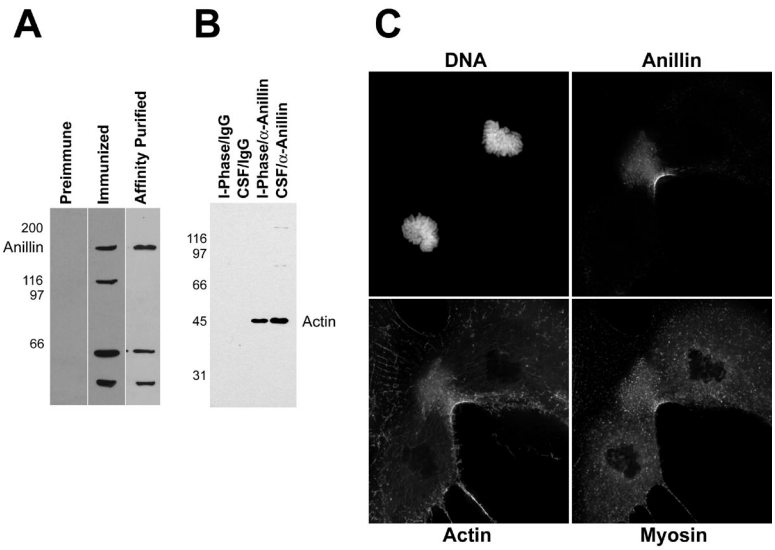

Figure 1. Characterization of *X. laevis* anillin. (A) Western blot of 20 μg of crude *X. laevis* egg extract with preimmune serum, immunized serum, and affinity-purified antibody. (B) Coimmunoprecipitation of anillin and actin from *Xenopus egg* extracts. Lane 1, interphase extract precipitated with rabbit IgG; lane 2, CSF extract precipitated with IgG; lane 3, interphase extract precipitated with anti-anillin; lane 4, CSF extract precipitated with anti-anillin. (C) immunofluorescence images XTC cells stained for DNA, anillin, actin, and myosin II.

Oligofectamine (Invitrogen) was diluted in 12 μl of Optimem-I. RNA was mixed with transfection reagent and after 20 min, the mixture was added directly to cells in the 24-well plate with 500 μl of DMEM containing 10% FBS. Cells were harvested at 48–72 h and either replated onto coverslips for microscopic analysis or lysed in extraction buffer (20 mM HEPES, pH 7.7, 0.5 M NaCl, 0.5% IGEPAL-CA630, 1 mM EDTA, 1 mM EGTA, 2 mM PMSF, and 10 μg/ml each of leupeptin, pepstatin, and chymostatin). For Western blotting, protein concentration was equalized, and 10-μg samples were blotted with anti-human anillin antibody (Oegema *et al*., 2000).

RESULTS

Characterization of Xenopus *Anillin*

Biochemical analysis of proteins involved in cytokinesis has proven difficult because their functions are often regulated during the cell cycle. We isolated the *Xenopus laevis* homolog of anillin to take advantage of the *Xenopus* egg extract system, in which cell cycle state can be controlled, for anillin biochemistry. *Xenopus* anillin is significantly homologous to both the human (59% overall identity) and *Drosophila* (27% overall identity) proteins. The most conserved part of the protein is the C-terminal PH domain that is 90% identical to the human PH domain and 60% identical to the *Drosophila* PH domain.

We generated antibodies to a fragment of the protein that contains the region of *Xenopus laevis* anillin homologous to the minimal actin-binding region mapped in *Drosophila* (Field and Alberts, 1995) (Figure 1A). Both *Drosophila* (Field and Alberts, 1995) and human anillin (Oegema *et al*., 2000) have been shown to bind F-actin, and we demonstrated this function to be conserved by both immunoprecipitation from *Xenopus* egg extracts (Figure 1B) and cosedimentation of purified proteins (our unpublished data). The antibody was used to localize anillin in *Xenopus* tissue culture cells (XTC). As previously described for both the *Drosophila* and human anillin, the protein localizes to the cleavage furrow in XTC cells (Figure 1C) and to the nucleus during interphase (our unpublished data). These data show that the *Xenopus* protein is indeed the ortholog of human and *Drosophila* anillin.

Discovery of Anillin-interacting Proteins by Affinity Chromatography

To gain insight into the function of anillin during cytokinesis, we isolated binding partners for anillin from *Xenopus* egg extracts arrested in mitosis and interphase. Full-length and PH domain-truncated *Xenopus* anillin proteins were expressed in Sf9 cells and purified. Expressed proteins were covalently attached to agarose beads and used as an affinity matrix. We prepared *Xenopus* extracts in interphase and in metaphase, applied these to anillin and control columns, washed, and eluted with increasing concentrations of NaCl. A prominent band of 200-kDa molecular mass bound specifically to the anillin columns but not to GST or *Xenopus* Polo kinase (PLX1) control columns. The interaction seemed cell cycle specific in that binding only occurred in metaphase extracts (Figure 2A).

The 200-kDa molecular mass of the interacting protein suggested that it was nonmuscle myosin II, the motor that drives cleavage furrow ingression and colocalizes with anillin at the contractile ring. We immunoblotted eluates from the affinity columns by using three different antibodies against nonmuscle myosin II that were raised to *Xenopus* myosin IIA heavy chain, *Xenopus* myosin IIB heavy chain, and a peptide sequence conserved between many myosins (Pinder *et al*., 1998) (Figure 2B). The identity of the 200-kDa band as nonmuscle myosin II heavy chain was confirmed by mass spectrometry. *Xenopus* extracts were prepared in the presence of the actin polymerization inhibitor cytochalasin D, and we observed very little actin binding to the columns in comparison with the myosin II that bound (<5% by staining intensity). This suggests that the interaction between anillin and nonmuscle myosin IIA and IIB is direct, rather than indirect through polymerized actin.

Anillin Binding Requires Myosin II Phosphorylation

We determined the sequence necessary for myosin II binding by truncating anillin from the carboxy terminus (Figure 3A). Fragments of anillin were expressed in Sf9 cells and coupled to solid support as described above. Mitotic *Xenopus* extracts were then applied to the columns and myosin II binding was assayed by electrophoresis and Coomassie staining of the column eluates (Figure 3B). Robust binding of myosin II to the affinity columns containing anillin fragments was observed as we truncated the protein from the carboxy terminus until the amino acids between positions 142 and 254 were deleted. The absence of these 112 amino acids reduced myosin II association to an amount comparable with control columns (Figure 2B, compare 1–142 to

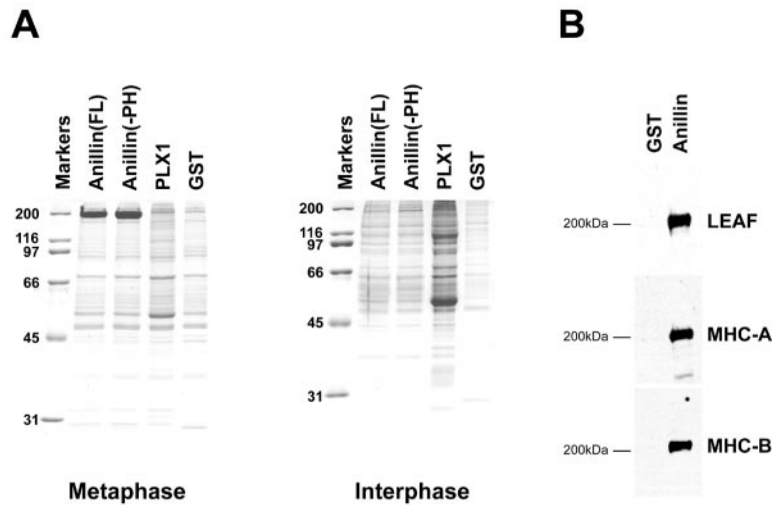

Figure 2. Anillin affinity chromatography. (A) Eluates from anillin (full length [FL] or without pleckstrin homology domain [−PH]), Polo kinase (PLX1), or GST columns. Left, cytostatic factor arrested extracts. Right, interphase extracts. (B) Eluates from GST and full-length anillin columns immunoblotted with antibodies to nonmuscle myosin II heavy chain.

PLX1). The PH domain of anillin showed no specific association with nonmuscle myosin II (Figure 3B, 973-1104). The region of the protein essential for myosin II binding contains several highly conserved amino acids that are invariant between the Human, *Xenopus*, and *Drosophila* proteins (Figure 3C). An expressed fragment encompassing only amino acids 142–254 of anillin was sufficient to bind myosin II (our unpublished data). This minimal fragment did not overlap with the region homologous to the minimal actin-binding domain of anillin, and we will refer to this region of anillin as the myosin-binding region.

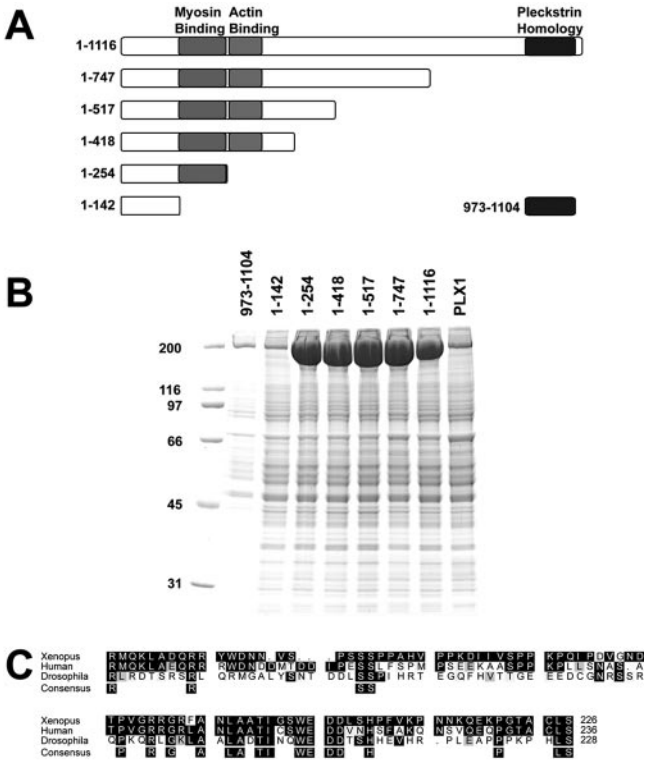

Figure 3. Delineation of myosin II binding region in anillin. (A) Schematic of anillin truncation fragments with minimal myosin binding region, region homologous to actin binding region, and pleckstrin homology domain highlighted. (B) Eluates from affinity columns for each of the fragments of anillin and Polo kinase (PLX1). Myosin II is the prominent band at 200 kDa. (C) Homology alignment of *Xenopus*, human, and *Drosophila* anillin in the myosin binding region.

We investigated whether the apparent mitosis-specific binding of myosin II to anillin was regulated by phosphorylation. Two key kinases, the cyclin-dependent kinase Cdk1 and Polo kinase, regulate cell cycle progression through mitosis and cytokinesis (Nigg, 1998; Murray, 2004). Furthermore, the contractile activity of myosin II during cytokinesis requires phosphorylation of the myosin II regulatory light chain by either myosin light chain kinase (MLCK), Rho-kinase, or Citron kinase (Yamakita *et al*., 1994; Amano *et al*., 1996; Yamashiro *et al*., 2003). We investigated whether any of these kinases controls the interaction between anillin and myosin II.

We purified human nonmuscle myosin II from platelets and either expressed or purified each kinase in an active form. Myosin II was incubated separately with each kinase in the presence of ATP to allow phosphorylation. We then assayed the interaction of phosphorylated myosin II with anillin by incubating anillin-coated or GST-coated beads with the kinase reaction, sedimenting the beads, and measuring the amount of myosin II bound to the beads. Only the reaction treated with MLCK showed binding of myosin II to anillin (Figure 4). No specific binding of myosin II was detected to the control GST beads (Figure S1), and all three kinases were independently demonstrated to be active (our unpublished data). These data suggest that MLCK phosphorylation of myosin II is required for anillin binding, and they also support our earlier conclusion that the interaction between anillin and myosin II is direct and not mediated by actin.

MLCK phosphorylates myosin regulatory light chain on amino acids serine 19 and threonine 18. Serine 19 phosphorylation results in a 1000-fold stimulation of the actin activated ATPase of myosin II and a shift in the equilibrium from the closed 10S conformation of myosin II to the open 6S conformation (Sellers, 1999). Our data suggest that anillin specifically recognizes myosin II that is activated for contraction. We suspect that what we initially interpreted as mitosis-specific binding of myosin II to anillin reflects the fact that we added phosphatase inhibitors to the mitotic *Xenopus* extracts to maintain a mitosis-like state during chro-

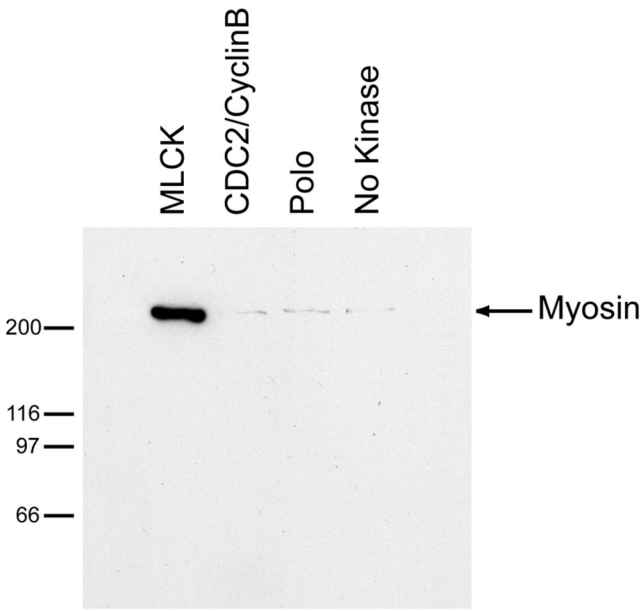

Figure 4. Anillin binds activated myosin II. Myosin II precipitation by anillin after myosin II phosphorylation by MLCK, Cdc2/CyclinB, Polo kinase, or no kinase.

matography (Felix *et al*., 1990). These phosphatase inhibitors likely stabilized myosin light chain phosphorylation, resulting in an increase in activated nonmuscle myosin II. In the cell, myosin–anillin interaction might be mostly restricted to mitosis and cytokinesis because anillin is largely sequestered in the nucleus in interphase.

High-Resolution Imaging of Anillin and Myosin II during Cytokinesis

Anillin and myosin II are known to approximately colocalize during cytokinesis (Oegema *et al*., 2000). To test for colocalization more critically, we used the myosin II inhibitor blebbistatin to block furrow contraction without disrupting the positioning of the contractile ring (Straight *et al*., 2003). Under these conditions, the arrested furrow accumulates most of the anillin and myosin II in the cell, and the extra time spent in cytokinesis may accentuate ordering of furrow components. An image taken through the center of a blebbistatin-treated cell that has entered cytokinesis phase shows a prominent midzone microtubule array, separated chromosomes and anillin positioned at the site of the contractile ring midway between the separated chromosomes (Figure 5A). Focal planes near the coverslip provided the best images of the contractile ring itself (Figure 5B). Spherical aberration is minimized near the coverslip; the furrow is flattened so structures are laid out in the x,y plane, and it is also possible that interactions with the substrate via adhesion proteins promote ordering of furrow components. In the substrate-opposed region of the furrow, anillin localizes to filamentous substructures within the contractile ring. Myosin II seems to decorate these anillin-rich filaments at alternating, approximately periodic intervals (Figure 5, B and C). These data are consistent with a direct physical interaction between the two proteins and suggest that filamentous anillin-myosin II assemblies are a building block for furrow organization. Prominent anillin-myosin II filaments are not observed in normally contracting furrows (Oegema *et al*., 2000; our unpublished data), but we believe this reflects difficulties in imaging, and a lesser degree of organization, in the dynamic, contracting furrow.

Analysis of Anillin and Myosin II Interactions during Cytokinesis

To explore the functional consequences of interactions between anillin and myosin II during cytokinesis, we turned to depletion experiments by using RNAi. We used two systems for this. *Drosophila* Kc167 tissue culture cells have the advantage that RNAi is very efficient and that all myosin II isoforms can be depleted with a single dsRNA duplex. Human HeLa cells have the advantage that their larger size facilitates cytological observation, especially during blebbistatin arrest (blebbistatin is inactive in *Drosophila* cells), and that we ultimately hope to understand human cytokinesis.

Addition of dsRNA derived from the *Drosophila* anillin cDNA to *Drosophila* Kc167 cells resulted in depletion of the

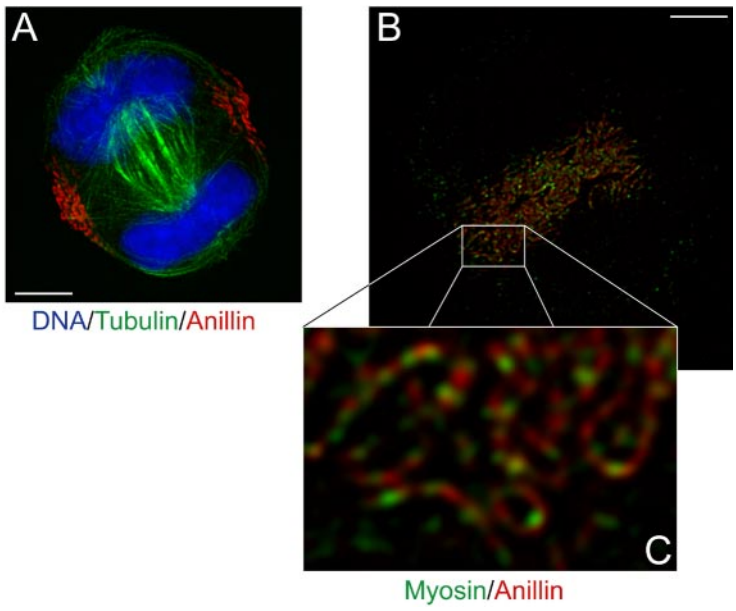

Figure 5. Myosin II and anillin organization in arrested contractile rings. (A) DNA, tubulin, and anillin staining in a blebbistatin-arrested HeLa cell. (B) Image plane at the coverslip surface in a blebbistatin-arrested HeLa cell stained for anillin and myosin II. (C) Enlarged view of B. Bars, 5 μm.

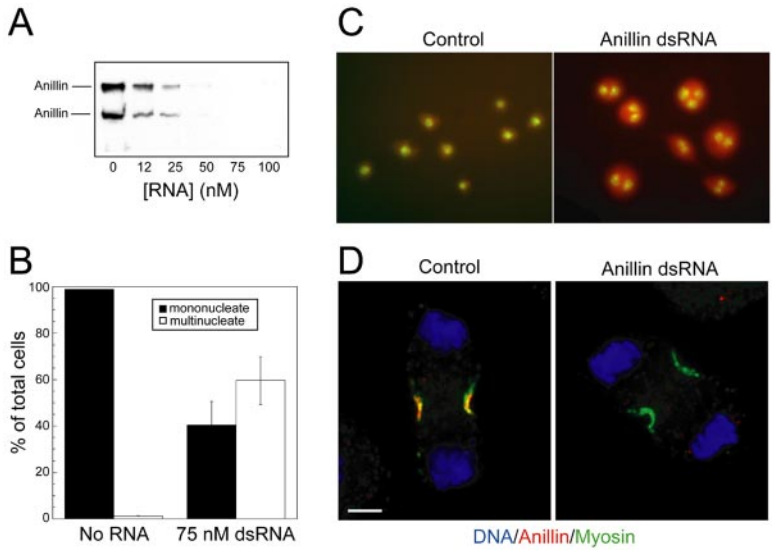

Figure 6. Depletion of anillin by dsRNA in *Drosophila* cells. (A) Western blot of anillin depletion at varying dsRNA concentrations. (B) Quantitation of multinucleate phenotype in untreated or 75 nM anillin dsRNA-treated cells stained for DNA and cell volume. (D) Image of *Drosophila* cell untreated or anillin dsRNA treated during cytokinesis stained for DNA, anillin, and myosin II. Bar, 5 μm.

anillin protein (Figure 6A). We assayed the frequency of multinucleate cell formation in cells depleted of anillin. More than 50% of all cells became multinucleate after 48 h of anillin depletion, suggesting a defect in cytokinesis (Figure 6, B and C), and consistent with previous observations (Somma *et al*., 2002). To investigate the effect of anillin depletion on nonmuscle myosin II, we stained cells undergoing cytokinesis for anillin and nonmuscle myosin II after dsRNA treatment. In control cells the two proteins colocalized in the furrow as expected (Figure 6D and Figure S2). After RNAi of anillin, anillin staining was completely missing in the cell. Nonmuscle myosin II still localized to the contractile ring, and anillin-free cleavage furrows still contracted (Figure 6D and Figure S3, a–c). We observed that control cells formed a focused band of myosin II at the contractile ring and an array of tightly bundled midzone microtubules (Figure S2), whereas some anillin-depleted cells exhibited poorly focused myosin II and disorganized midzone microtubules (Figure S3, d–f). Anillin depletion may have some effect on furrow assembly, but myosin II is still able to target to the furrow and contract. Thus, the primary defect in anillin-depleted cells is the failure to complete cytokinesis.

We next tested whether depletion of myosin II affects anillin recruitment or localization. We depleted myosin II from *Drosophila* Kc167 cells by treatment with dsRNA recognizing the *Drosophila* nonmuscle myosin II heavy chain (Figure 7A). The majority of myosin II-depleted cells became multinucleate (Figure 7, B and C). A discrete equatorial band of anillin assembled between the separating chromosomes in anaphase myosin II-depleted cells, and this band was remarkably similar to the furrow of control cells early in cytokinesis in terms of morphology and intensity. However this myosin II free furrow was never observed to contract (Figure 7D). Thus, myosin II is not required for targeting of anillin to the furrow, and the two proteins can target independently. Myosin II depletion specifically affects contraction of the furrow, as expected, without disrupting its positioning, or assembly of another component.

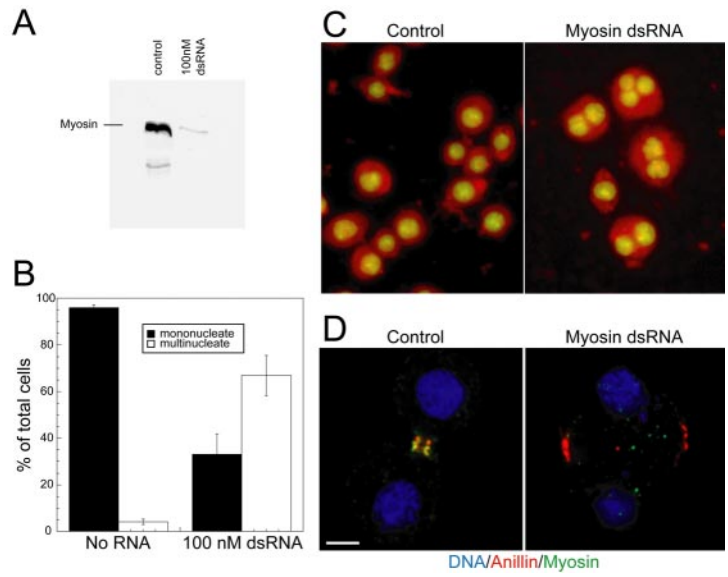

Figure 7. Depletion of myosin II by dsRNA in *Drosophila* cells. (A) Western blot of myosin II after control and 100 nM myosin II dsRNA treatment. (B) Quantitation of multinucleate phenotype in untreated or myosin II dsRNA-treated cells. (C) DNA staining of multinucleate cells in control or myosin II dsRNA-treated cells. (D) Image of control or myosin II dsRNA-treated cells during cytokinesis stained for DNA, anillin, and myosin II. Bar, 5 μm.

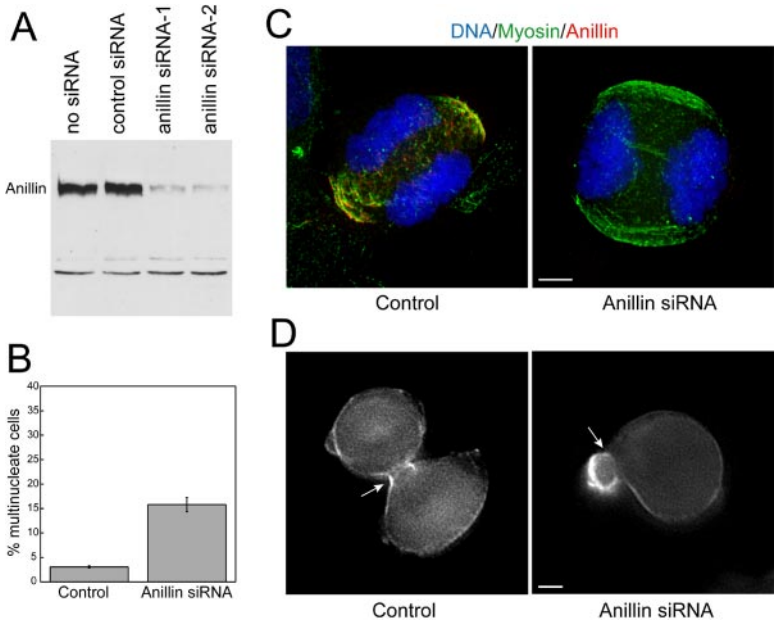

Figure 8. Depletion of anillin by siRNA in HeLa cells. (A) Western blot with anti-anillin of whole cell lysates after treatment with no RNA, control siRNA, or siRNA directed against human anillin. (B) Frequency of multinucleation in control or siRNA-treated HeLa cells. (C) immunofluorescence staining of DNA (blue), anillin (green), and myosin II (red) in HeLa cells treated with control or anillin siRNA. (D) Single frames of YFP-Myosin fluorescence from Movie S4, control, and Movie S8, anillin siRNA. White arrow indicates position of contractile ring. Bars, 5 μm.

Anillin Constrains Myosin II Contractility to the Cleavage Furrow at the End of Cytokinesis

Treatment of HeLa cells with either of two different siRNAs directed against human anillin resulted in depletion of the anillin protein (Figure 8A). Treatment with no siRNA or a nonspecific siRNA had no effect. The anillin siRNA treatment resulted in an increase in binucleate cells, suggesting a cytokinesis defect like that observed in *Drosophila* tissue culture (Figures 6 and 8B). The binucleate frequency was not as high in HeLa cells as it was in *Drosophila*, suggesting that either the siRNA treatment was less efficient at depletion of the anillin protein or that vertebrate cells use additional mechanisms to ensure completion of cytokinesis.

We examined the localization of nonmuscle myosin II during HeLa cell cytokinesis after depletion of anillin, by using blebbistatin to block contraction and facilitate detailed structural observation. As we observed in *Drosophila* cells, myosin II is able to properly localize to the contractile ring in the absence of anillin (Figure 8C). We could not detect any gross abnormalities in the localization of myosin II at the cleavage furrow in the absence of anillin. Without anillin staining as a visual cue, no clear relationship between adjacent myosin II foci could be established, and thus we were unable to determine whether the more detailed organization of myosin along anillin seen in Figure 5C was perturbed. Furthermore, cells that were not treated with blebbistatin but were depleted of anillin were able to initiate furrow contraction. We were unable to deplete myosin II to ask whether anillin can target independently of myosin II.

We used live cell microscopy to dissect the role of anillin in the completion of cytokinesis. We cotransfected cells with siRNA to deplete anillin and with a YFP fusion to the regulatory light chain of nonmuscle myosin II to monitor myosin II dynamics. We imaged cytokinesis in these cells both by differential interference contrast and epifluorescence microscopy. Cells that were cotransfected with YFP-myosin RLC and nonspecific siRNA or no siRNA proceeded through cytokinesis normally (Movies S1 and S3). Myosin II became enriched in the cytokinetic ring as the cell contracted to form two symmetrical daughter cells (Figure 8D, control, and Movies S3 and S4). Contractility was well controlled in these cells, causing contraction of the furrow itself and some blebbing but not dramatic shape changes of the incipient daughter cells. In the anillin-depleted cells, furrow contraction began normally and myosin II localized to the furrow as it did in control cells. After the furrow had constricted to approximately one-third of its original diameter (35.7 $\pm$ 2.5%, 13.4 $\pm$ 1.2 min after anaphase initiation), cells began to contract abnormally. The incipient daughter cells were observed to change diameter dramatically, growing on one side and shrinking on the other, as the cytoplasm was extruded back and forth through the contractile ring (Movies S5 and S7). The localization of YFP-myosin RLC was no longer confined to the contractile ring. YFP-myosin RLC was also concentrated at sites in the cortex where abnormal contraction was occurring (Figure 8D, anillin siRNA, and Movies S6 and S8). During abnormal contractility, the contractile ring was sometimes displaced to the side of the two daughter nuclei (Movies S5 and S7). Abnormal contraction eventually subsided and the cleavage furrow regressed resulting in cytokinesis failure.

DISCUSSION

Anillin Is a Multifunctional Cytoskeletal Element

We show that the anillin protein is a multifunctional component of the cytoskeleton that is recruited to the furrow early in cytokinesis but functions primarily late in cytokinesis to focus contractility at the furrow. Anillin is known to directly interact with actin and contribute to the organization of the septin complex along actin filaments (Field and Alberts, 1995; Kinoshita *et al*., 2002). We show that anillin also directly interacts with nonmuscle myosin II. This interaction with myosin II depends upon phosphorylation of myosin II regulatory light chain by MLCK, suggesting that anillin only associates with active myosin II.

We tested whether anillin functions in cytokinesis to recruit activated myosin II to the cleavage furrow. Our anillin depletion data in vivo rule out this simple model because myosin II is able to localize to the division site and promote furrow contraction with normal timing in the absence of anillin. Oegema *et al*. (2000) observed reduction of the initial

rate of furrow contraction after inhibiting anillin by antibody injections, but our depletion data suggest this may have been due to the presence of antibody in the furrow rather than anillin removal. We also found that anillin targets to the furrow normally when myosin II is depleted, although in this case contraction is completely inhibited. Those data are consistent with previous pharmacological studies where we showed that inhibition of kinases that regulate cytokinesis interfere with targeting of myosin II, but not of anillin, to the furrow (Straight *et al.*, 2003). It will be interesting to test in the future where the pathways that target myosin II and anillin diverge. Both require the continual presence of microtubules (Straight *et al.*, 2003) and probably also activated Rho (Somma *et al.*, 2002) to target normally.

Anillin Focuses Myosin II Contractility Late in Cytokinesis

The primary defect we observe in cells that lack anillin is a delocalization of contraction at the end of cytokinesis. Observation of myosin II dynamics in anillin-depleted cells revealed that myosin II was no longer constrained to the contractile ring as it was in control cells and instead could be found in the cell cortex concomitant with aberrant cell contraction. This aberrant contraction often resulted in both mispositioning of the cleavage furrow to yield binucleate cells or to furrow regression and thus binucleation. We were not able to deplete all of the anillin by RNAi in human cells, thus complete depletion or inhibition of the anillin protein may result in an even more severe cytokinesis phenotype. It is not clear whether the phenotype we observe represents extra contraction, for example, due to hyperactivation of myosin II, or relocalization of contraction due to mislocalization of active myosin II to ectopic sites. Distinguishing these hypotheses will require measuring contractile properties of the cortex at different positions. Because anillin is restricted to the contractile ring in unperturbed cells, it is unlikely that anillin outside the furrow inhibits myosin II. Overall, our data point to a model whereby anillin binding to activated myosin II restricts its activity to the furrow until cytokinesis can complete. Anillin is retained in the fully contracted furrow much longer than myosin II, and it is also present in intracellular bridges that are no longer contracting (Field and Alberts, 1995). An extension of our model proposes that loss of myosin II from the fully contracted furrow is promoted by cell cycle-dependent modification of anillin and/or myosin, such as dephosphorylation of myosin regulatory light chain.

Control of Cytokinesis by Anillin

Several lines of evidence suggest that anillin controls, or at least coordinates multiple aspects of cytokinesis. Two anillin-related proteins in yeast, Mid1 and Mid2, organize distinct steps during cytokinesis. The Mid1 protein, like anillin, relocalizes from the nucleus to the contractile ring early in cytokinesis (Sohrmann *et al.*, 1996; Wu *et al.*, 2003). Mid1 mutants are defective in septum placement and formation (Sohrmann *et al.*, 1996) and overexpression of Mid1 disrupts cytokinesis (Bahler *et al.*, 1998; Paoletti and Chang, 2000). Several important differences exist between Mid1 and anillin. Mid1 is not essential, does not require actin filaments or microtubules to be maintained at the division site, and does not contract with the actomyosin contractile ring (Paoletti and Chang, 2000; Wu *et al.*, 2003). However, Mid1 is important for the initial organization of myosin II at the contractile ring and can interact with myosin II (Wu *et al.*, 2003; Motegi *et al.*, 2004). A second anillin-like protein in fission yeast, Mid2, performs other functions that depend on anillin in metazoan cells. In particular, Mid2 organizes septins in fission yeast and is necessary for proper cell separation (Berlin *et al.*, 2003; Tasto *et al.*, 2003), whereas metazoan anillin binds directly to septins (Kinoshita *et al.*, 2002) and participates in targeting septins to the cortex (Oegema *et al.*, 2000). Mid2 mutant cells have no defect in myosin II localization or contraction at the end of cytokinesis (Berlin *et al.*, 2003). Thus, metazoan anillin may encompass the activities of both Mid1 and Mid2. We speculate that the functions of anillin may be split in fission yeast because of the different mechanical requirements for cytokinesis. In yeast, remodeling of the cell wall may be the primary requirement for cytokinesis, whereas cytokinesis in metazoan animals is dominated by the need to physically constrict the equator of the dividing cell. In budding yeast, the mechanical requirements are different again, because the cell division site is predetermined at a narrow constriction. In that system, myosin II targets very early and no anillin-like proteins have been identified (Field *et al.*, 1999).

Anillin is known to be essential for the completion of cytokinesis in vertebrate cells (Oegema *et al.*, 2000) and in *Drosophila* (Somma *et al.*, 2002). Anillin's interaction with both the septin complex and with filamentous actin may be required for cell abscission. Myosin II leaves the contractile ring late in cytokinesis, but anillin persists at these contracted furrows (Figure S2), suggesting that anillin's role in the completion of cytokinesis may only be partially explained by its interaction with myosin II. Our results suggest an early role for anillin in cytokinesis to properly organize the contractile ring and a late function for anillin in restricting myosin II contraction to the furrow. In *Drosophila* embryos expressing mutant anillin, actin, and myosin II are disorganized during cellularization (Thomas and Wieschaus, 2004; Field, unpublished data). This may reflect an analogous role for anillin in organizing myosin II at the cellularization front as well as at the contractile ring during cytokinesis.

The events of mitosis are temporally coupled by the activities of protein kinases that drive the cell cycle and the proteasome that inactivates these kinases and degrades other proteins involved in mitosis. We have previously shown a role for proteolysis in the disassembly of the contractile ring (Straight *et al.*, 2003) in vertebrate cells. Possible substrates for this proteolysis are anillin and the cell cycle kinase Polo. In yeast, Mid2 is degraded by ubiquitin-mediated proteolysis (Tasto *et al.*, 2003), it will be interesting to determine whether in somatic cells anillin is degraded upon mitotic exit, although we observe no change in anillin levels during the metaphase-to-interphase transition in *Xenopus* egg extracts. Mid1 is controlled by the activity of Polo kinase in fission yeast. In *Xenopus* extracts, anillin is rapidly dephosphorylated as cells exit mitosis and is efficiently phosphorylated by Polo kinase in vitro (our unpublished data). Regulation of anillin by phosphorylation may provide another effective means of coupling the early and late events of cytokinesis to the cell cycle.

Our results demonstrate a role for anillin in localizing the contractile activity of myosin in addition to anillin's previously identified functions in binding actin and organizing the septins. Thus, anillin seems to be a central factor for coupling the filament systems that interact during cytokinesis. Understanding how proteins such as anillin dynamically organize the cytoskeletal and regulatory networks that are integrated to accomplish cytokinesis will be key to understanding the process of cell division.

ACKNOWLEDGMENTS

We thank A. Kumagai and W. Dunphy for the baculovirus to express Polo kinase; Noel Peterson and Randy King for purified Cdc2/CyclinB; Robert Adelstein for the *Xenopus* nonmuscle myosin II heavy chain clone; Fei Wang, Mary Ann Conti, and Jim Sellers for the Human heavy meromyosin and essential and regulatory light chain viruses; and Steve Gygi for mass spectrometry identification. We thank Amy Maddox for advice on siRNA and for comments on the manuscript. A.F.S. was supported by the Cancer Research Fund of the Damon Runyon-Walter Winchell Foundation. This work was supported by the National Institute of General Medical Sciences grant GM-023928.

REFERENCES

Amano, M., Ito, M., Kimura, K., Fukata, Y., Chihara, K., Nakano, T., Matsuura, Y., and Kaibuchi, K. (1996). Phosphorylation and activation of myosin by Rho-associated kinase (Rho-kinase). J. Biol. Chem. *271*, 20246–20249.

Bahler, J., Steever, A. B., Wheatley, S., Wang, Y., Pringle, J. R., Gould, K. L., and McCollum, D. (1998). Role of polo kinase and Mid1p in determining the site of cell division in fission yeast. J. Cell Biol. *143*, 1603–1616.

Berlin, A., Paoletti, A., and Chang, F. (2003). Mid2p stabilizes septin rings during cytokinesis in fission yeast. J. Cell Biol. *160*, 1083–1092.

Bhatia-Dey, N., Taira, M., Conti, M. A., Nooruddin, H., and Adelstein, R. S. (1998). Differential expression of non-muscle myosin heavy chain genes during *Xenopus* embryogenesis. Mech. Dev. *78*, 33–36.

Daniel, J. L., and Sellers, J. R. (1992). Purification and characterization of platelet myosin. Methods Enzymol. *215*, 78–88.

De Lozanne, A., and Spudich, J. A. (1987). Disruption of the *Dictyostelium myosin* heavy chain gene by homologous recombination. Science *236*, 1086–1091.

Felix, M. A., Cohen, P., and Karsenti, E. (1990). Cdc2 H1 kinase is negatively regulated by a type 2A phosphatase in the *Xenopus* early embryonic cell cycle: evidence from the effects of okadaic acid. EMBO J. *9*, 675–683.

Field, C., Li, R., and Oegema, K. (1999). Cytokinesis in eukaryotes: a mechanistic comparison. Curr. Opin. Cell Biol. *11*, 68–80.

Field, C. M., and Alberts, B. M. (1995). Anillin, a contractile ring protein that cycles from the nucleus to the cell cortex. J. Cell Biol. *131*, 165–178.

Glotzer, M. (2001). Animal cell cytokinesis. Annu. Rev. Cell Dev. Biol. *17*, 351–386.

Kelley, C. A., Sellers, J. R., Gard, D. L., Bui, D., Adelstein, R. S., and Baines, I. C. (1996). *Xenopus* nonmuscle myosin heavy chain isoforms have different subcellular localizations and enzymatic activities. J. Cell Biol. *134*, 675–687.

Kinoshita, M., Field, C. M., Coughlin, M. L., Straight, A. F., and Mitchison, T. J. (2002). Self- and actin-templated assembly of mammalian septins. Dev. Cell *3*, 791–802.

Knecht, D. A., and Loomis, W. F. (1987). Antisense RNA inactivation of myosin heavy chain gene expression in *Dictyostelium discoideum*. Science *236*, 1081–1086.

Mabuchi, I., and Okuno, M. (1977). The effect of myosin antibody on the division of starfish blastomeres. J. Cell Biol. *74*, 251–263.

Mansfield, S. G., al-Shirawi, D. Y., Ketchum, A. S., Newbern, E. C., and Kiehart, D. P. (1996). Molecular organization and alternative splicing in zipper, the gene that encodes the *Drosophila* non-muscle myosin II heavy chain. J. Mol. Biol. *255*, 98–109.

Motegi, F., Mishra, M., Balasubramanian, M. K., and Mabuchi, I. (2004). Myosin-II reorganization during mitosis is controlled temporally by its dephosphorylation and spatially by Mid1 in fission yeast. J. Cell Biol. *165*, 685–695.

Murray, A. W. (1991). Cell cycle extracts. In: *Xenopus laevis*: Practical Uses in Cell and Molecular Biology, vol. 36, ed. H. B. Peng, San Diego, CA; Academic Press. 581–605.

Murray, A. W. (2004). Recycling the cell cycle: cyclins revisited. Cell *116*, 221–234.

Nigg, E. A. (1998). Polo-like kinases: positive regulators of cell division from start to finish. Curr. Opin. Cell Biol. *10*, 776–783.

Oegema, K., Savoian, M. S., Mitchison, T. J., and Field, C. M. (2000). Functional analysis of a human homologue of the *Drosophila* actin binding protein anillin suggests a role in cytokinesis. J. Cell Biol. *150*, 539–552.

Paoletti, A., and Chang, F. (2000). Analysis of mid1p, a protein required for placement of the cell division site, reveals a link between the nucleus and the cell surface in fission yeast. Mol. Biol. Cell *11*, 2757–2773.

Pardee, J. D., and Spudich, J. A. (1982). Purification of muscle actin. Methods Enzymol. *85*, 164–181.

Pato, M. D., Sellers, J. R., Preston, Y. A., Harvey, E. V., and Adelstein, R. S. (1996). Baculovirus expression of chicken nonmuscle heavy meromyosin II-B. Characterization of alternatively spliced isoforms. J. Biol. Chem. *271*, 2689–2695.

Pinder, J. C., Fowler, R. E., Dluzewski, A. R., Bannister, L. H., Lavin, F. M., Mitchell, G. H., Wilson, R. J., and Gratzer, W. B. (1998). Actomyosin motor in the merozoite of the malaria parasite, *Plasmodium falciparum*: implications for red cell invasion. J. Cell Sci. *111*, 1831–1839.

Pollard, T. D. (1982). Purification of nonmuscle myosins. Methods Enzymol. *85*, 331–356.

Rappaport, R. (1996). Cytokinesis in Animal Cells, Cambridge, United Kingdom Cambridge University Press.

Sellers, J. R. (1999). Myosins, Oxford, NY: Oxford University Press.

Sohrmann, M., Fankhauser, C., Brodbeck, C., and Simanis, V. (1996). The dmf1/mid1 gene is essential for correct positioning of the division septum in fission yeast. Genes Dev. *10*, 2707–2719.

Somma, M. P., Fasulo, B., Cenci, G., Cundari, E., and Gatti, M. (2002). Molecular dissection of cytokinesis by RNA interference in *Drosophila* cultured cells. Mol. Biol. Cell *13*, 2448–2460.

Straight, A. F., Cheung, A., Limouze, J., Chen, I., Westwood, N. J., Sellers, J. R., and Mitchison, T. J. (2003). Dissecting temporal and spatial control of cytokinesis with a myosin II Inhibitor. Science *299*, 1743–1747.

Straight, A. F., and Field, C. M. (2000). Microtubules, membranes and cytokinesis. Curr. Biol. *10*, R760–R770.

Tasto, J. J., Morrell, J. L., and Gould, K. L. (2003). An anillin homologue, Mid2p, acts during fission yeast cytokinesis to organize the septin ring and promote cell separation. J. Cell Biol. *160*, 1093–1103.

Thomas, J. H., and Wieschaus, E. (2004). src64 and tec29 are required for microfilament contraction during *Drosophila* cellularization. Development *131*, 863–871.

Walsh, M. P., Hinkins, S., Dabrowska, R., and Hartshorne, D. J. (1983). Smooth muscle myosin light chain kinase. Methods Enzymol. *99*, 279–288.

Wang, F., Harvey, E. V., Conti, M. A., Wei, D., and Sellers, J. R. (2000). A conserved negatively charged amino acid modulates function in human nonmuscle myosin IIA. Biochemistry *39*, 5555–5560.

Wheatley, S. P., O'Connell, C. B., and Wang, Y. (1998). Inhibition of chromosomal separation provides insights into cleavage furrow stimulation in cultured epithelial cells. Mol. Biol. Cell *9*, 2173–2184.

Wu, J. Q., Kuhn, J. R., Kovar, D. R., and Pollard, T. D. (2003). Spatial and temporal pathway for assembly and constriction of the contractile ring in fission yeast cytokinesis. Dev. Cell *5*, 723–734.

Yamakita, Y., Yamashiro, S., and Matsumura, F. (1994). In vivo phosphorylation of regulatory light chain of myosin II during mitosis of cultured cells. J. Cell Biol. *124*, 129–137.

Yamashiro, S., Totsukawa, G., Yamakita, Y., Sasaki, Y., Madaule, P., Ishizaki, T., Narumiya, S., and Matsumura, F. (2003). Citron kinase, a Rho-dependent kinase, induces di-phosphorylation of regulatory light chain of myosin II. Mol. Biol. Cell *14*, 1745–1756.